ACADEMIA
ENVIRONMENTAL SCIENCES &
SUSTAINABILITY

Research Article
Published: 2025-04-07
https://doi.org/10.20935/AcadEnvSci7624

Does drone-facilitated revegetation work? A case study from Taiwan

Maria Gomez Saldarriaga[1,*], Marcus Lee[2], Samantha Farquhar[1]

Academic Editor: Kuok Ho Daniel Tang

Abstract

Unmanned aerial vehicle (UAV) or drone technology has gained significant traction in ecological restoration projects, particularly in revegetation efforts aimed at stabilizing degraded landscapes. Despite this growing interest, empirical data on the effectiveness of drone-based reseeding remain scarce. This study addresses this gap by investigating a core question—"Does drone-facilitated revegetation work?"—using a case study of three landslide-affected sites in Taiwan that underwent UAV seeding, alongside a fourth, untreated control site. We employed a dual remote-sensing approach using Google Earth Engine (GEE), leveraging both the Normalized Difference Vegetation Index (NDVI) and the Enhanced Vegetation Index (EVI) to quantify vegetation health before and after drone interventions. Results indicate that two of the three treatment sites showed notable improvements in NDVI and EVI, suggesting successful vegetation establishment, whereas the third site exhibited a less favorable response, highlighting the importance of site-specific conditions. The control site underwent only minimal natural recovery by comparison. These findings underscore the potential advantages of UAV-assisted seeding in challenging terrains and offer insights into how future drone-based revegetation projects might be refined for greater efficacy.

Keywords: *landslides, Taiwan, Google Earth Engine (GEE), Landsat, Sentinel-2, aerial restoration, unmanned aerial vehicle (UAV), restoration*

Citation: Saldarriaga MG, Lee M, Farquhar S. Does drone-facilitated revegetation work? A case study from Taiwan. *Academia Environmental Sciences and Sustainability* 2025;2. https://doi.org/10.20935/AcadEnvSci7624

1. Introduction

Restoration ecology is a multidisciplinary field that seeks to rehabilitate degraded ecosystems by applying ecological principles to restore their natural, historical, or desired conditions [1]. A critical tool in restoration efforts is revegetation, which involves reintroducing plant species—often native—into landscapes that have suffered environmental disturbances [2]. By fostering diverse and sustainable plant communities, revegetation helps stabilize soil, prevent erosion, provide habitat for wildlife, and enhance ecosystem services.

As restoration ecology has advanced, so too have revegetation techniques, evolving from traditional manual planting to large-scale aerial seeding. Several countries have experimented with helicopter-based or plane-based revegetation to address challenges in degraded landscapes [3, 4]. While aerial seeding offers large-scale coverage, it is not without limitations. Helicopter-based or plane-based revegetation is costly, logistically complex, and limited in precision. Issues such as airflow disturbances, operator visibility constraints, and inefficient seed distribution make it less effective in small, fragmented, or topographically complex areas. Manual planting, though effective, is often impractical due to high labor costs, time requirements, and accessibility challenges in remote regions.

Recent advancements in technology have introduced drones or unmanned aerial vehicles (UAVs) as a promising alternative for revegetation [5]. UAVs offer greater mobility, remote operation, and cost-effectiveness, particularly for small-scale projects or inaccessible terrains. In drone-facilitated revegetation, UAVs distribute seeds from the air, aiming for natural germination and ecosystem regeneration. This method has been heralded for its efficiency—potentially reducing labor needs by up to tenfold—and for improving safety in hazardous environments [6].

However, skepticism remains regarding its effectiveness. Despite the growth of drone forestry and revegetation companies worldwide, empirical validation of drone-based seeding remains limited. Castro et al. [7] highlighted the scarcity of scientific assessments measuring UAV revegetation success. Similarly, Mohan et al. [6] found that one drone-based revegetation company reported only a 20% seed survival rate, underscoring the need for further refinement. While theoretical research has explored UAV-assisted revegetation, including deep learning applications to enhance seed dispersal accuracy [8], the real-world success of drone-facilitated revegetation remains largely untested [5].

Given this knowledge gap, rigorous field studies are needed to assess the performance of drone-based revegetation sites. This research aims to answer the simple question, "Does drone-

[1]Integrated Coastal Sciences PhD program, East Carolina University, Greenville, NC, 27858, USA.
[2]Yale College, Yale University, New Haven, CT, 06520, USA.
*email: gomezsaldarriagam14@students.ecu

facilitated revegetation work?", by evaluating the effectiveness of a UAV-assisted revegetation effort that occurred in Taiwan. By monitoring vegetation recovery and ecological outcomes, this study aims to contribute to the growing but still limited body of literature on this emerging technology.

2. Materials and methods

2.1. Background and study areas

Taiwan, an island in East Asia, is characterized by rugged and mountainous terrain covered with abundant forests. Due to its topography, climate, and seismic activity, landslides are a frequent occurrence. In response, the Taiwanese government often undertakes revegetation efforts in landslide-affected areas to stabilize the land. However, accessing these collapsed areas is often difficult and can be quite costly.

Before the advent of drones, Taiwan relied on helicopters for planting operations in these remote locations [9]. In 2019, the Taiwan Forestry Bureau (TFB) experimented with using drones to revegetate landslide-affected areas by dispersing seeds over three such sites. Specifically, the TFB utilized an AG3 drone developed by AGROBOT. This rotary-wing drone features vertical takeoff and landing capabilities, a cruising speed of 60–120 km/h, and a minimum endurance of 60 min when fully loaded. It can operate at altitudes up to 3,000 m with a maximum flight radius of 30 km [10].

Plant species for UAV aerial seeding were selected based on government-established criteria prioritizing the following attributes:

- Native (indigenous) plants supplemented by domesticated non-native species.
- Pioneer herbaceous and dominant species that thrive in natural succession, reproduce easily, and grow rapidly.
- Tree species with abundant seed supplies suitable for afforestation on abandoned lands.
- Woody plants with strong disaster prevention characteristics suitable for landslide-affected areas.
- Grasses or legumes that quickly establish vegetation, have high seed availability, and pose no ecological harm.
- Pioneer grass seeds for coverage, prioritizing species that are locally available, have been used in Taiwan for disaster prevention for over 20 years and are readily purchasable in large quantities.

Based on these criteria, the selected herbaceous plants included tall fescue (*Festuca arundinacea*) and Bahia grass (*Paspalum notatum*), while the selected woody plants included Chinese bushclover (*Sericea lespedeza*), Formosan alder (*Alnus formosana*), Formosa acacia (*Acacia confusa*), shrubby bushclover (*Lespedeza bicolor*), and Roxburgh sumac (*Rhus chinensis* var. *roxburghii*) [10–12]. The planting granules were designed to optimize seed germination and growth while maintaining a lightweight, water-retaining, and cost-effective composition. The final formulation consisted of clay soil, slow-release fertilizer, and culture soil as growth substrates; red jade soil as a base material; pulp fiber as a covering material; and an agglomerating agent as a cementitious binder. The granules comprised approximately 13% seed material, with the remaining mass consisting of fertilizer, soil, and binding agents. Each granule weighed approximately 4.5–5 g [10].

The total cost of this experimental UAV-based seeding, including both material and operational expenses, was estimated at 1.1 million NTD (approximately 33,200 USD) per hectare. This approach was deemed more efficient than manual seeding methods, which were estimated to cost 3 million NTD per hectare [10].

Ultimately, three landslide-affected areas underwent this drone-facilitated revegetation effort (**Figure 1**). For each site, three treatments were administered over a 2.5-month period. During each treatment, the drone performed approximately 30 flights, dispersing an estimated 700,000 seeds per site [13, 14]. Study Area 1 experienced a landslide in 2012 during Typhoon Saola, which resulted in slope collapse and downstream debris flow. Study Area 2 suffered a similar fate due to Typhoon Mindulle in 2004, while Study Area 3 was affected by Typhoon Morakot in 2009, causing damage to road infrastructure [10, 11, 15].

Additionally, for the purposes of this study, a fourth site, Study Area 4, was included as the control (**Figure 1**). As identified through the NASA COOLR database [16], this site is located in the remote Babokulu Mountain area, which is frequented by hikers. It experienced a landslide in 2017 but did not undergo any significant restoration efforts. The characteristics and locations of all study areas are presented in **Table 1**.

2.2. Overview of remote-sensing methods

This study combined multiple remote-sensing approaches to evaluate vegetation recovery after the drone intervention. Long-term trends were examined using Landsat imagery and calculating a Normalized Difference Vegetation Index (NDVI) time series, spanning nearly two decades, to capture broad-scale changes and the establishment of species with longer germination periods. Short-term changes were assessed using Sentinel-2 imagery, focusing on Enhanced Vegetation Index (EVI) to detect immediate, finer-scale responses to treatment. This short-term analysis included pre- and post-treatment spatial change assessments and employed statistical methods such as empirical cumulative distribution functions (ECDFs), probability density functions (PDFs), and Kolmogorov–Smirnov (K-S) tests, to quantify the extent of vegetation recovery in both intervention and control sites. Additionally, we used Sentinel-2 imagery to analyze EVI over a longer time scale pre- and post-intervention by generating scatter plots. Ultimately, by capitalizing on Landsat's extensive temporal coverage and Sentinel-2's finer spatial detail, a more precise and comprehensive analysis of vegetation dynamics could be complete.

2.2.1. Landsat Normalized Difference Vegetation Index analysis

To monitor the long-term success of drone revegetation events, NDVI analysis was conducted for each study area. Landsat surface reflectance (SR) data from Collections 5, 7, 8, and 9 were accessed and processed using Google Earth Engine (GEE) [17]. The dataset was filtered to include imagery from the years 2000 to 2024 with a maximum cloud cover threshold of 20%. To ensure consistency across different Landsat sensors, SR values were standardized using appropriate scaling factors for optical and thermal bands. Cloud and shadow pixels were masked using the QA_PIXEL band, retaining only high-quality imagery. Additionally, to correct for seasonal variations, imagery was restricted to a consistent time window from April 1 to July 31 each year. This approach minimized phenological differences and ensured comparability across years.

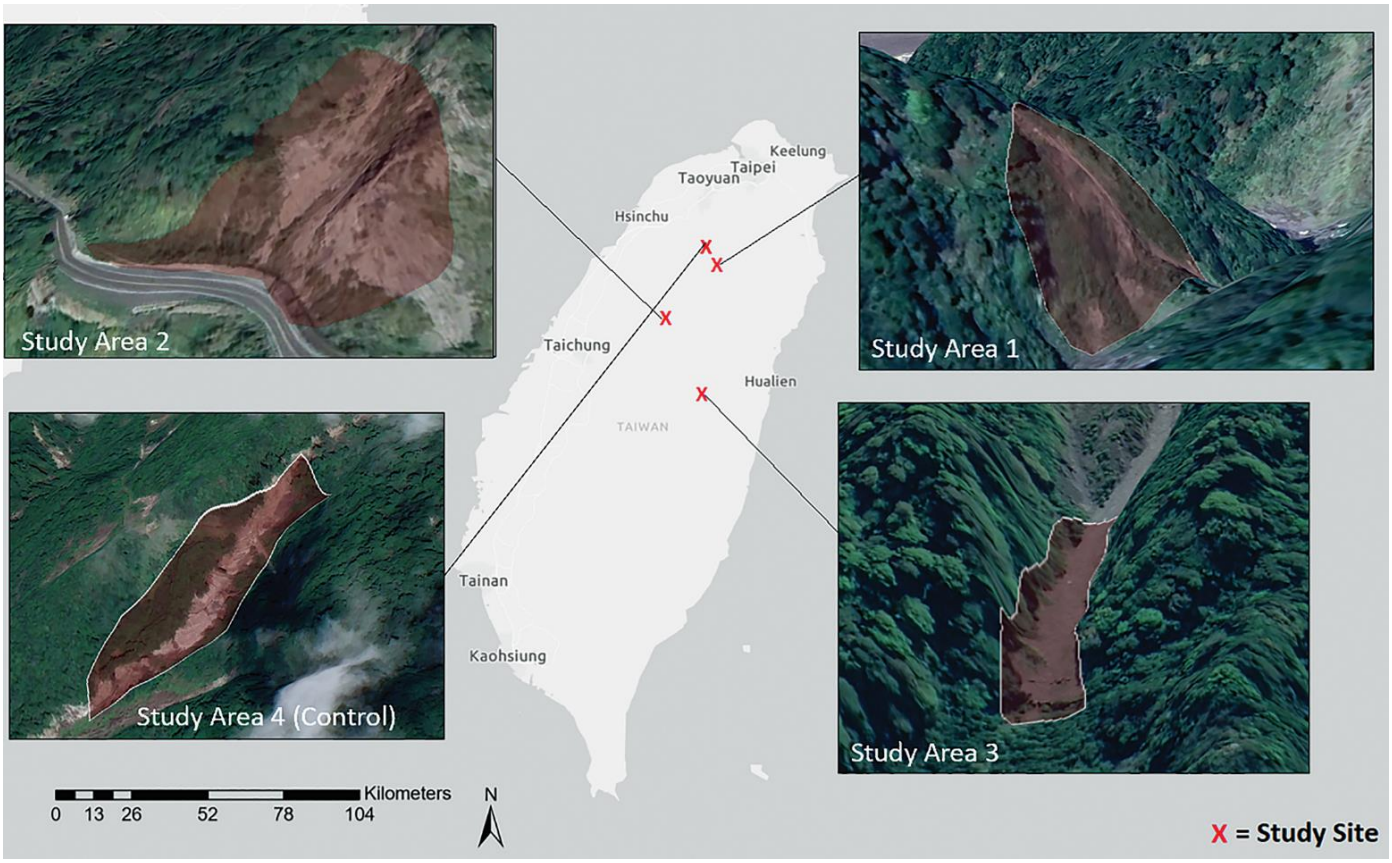

Figure 1 • Study map and satellite imagery of each drone-facilitated revegetation area and the Control Area.

Table 1 • Location and characteristics of each drone-facilitated revegetation area

Study area number	Area (m^2)	Average slope	Slope direction	Point location latitude	Point location longitude	Date of landslide event	Months of drone revegetation event
1	3,286	−83.3%	East	24°31'42.59"N	121°27'27.43"E	August 8, 2012	April 2019 June 2019 June 2019
2	7,097	−51.3%	Northwest	24°14'51.18"N	121°09'53.00"E	July 2, 2004	April 2019 June 2019 June 2019
3	5,423	−78.2%	South	23°57'31.75"N	121°09'3.20"E	August 7, 2009	April 2019 June 2019 June 2019
4 (Control)	1,3749	−45.4%	Southeast	24°35'59.81"N	121°25'40.08"E	May 28, 2017	N/A

To account for terrain-induced variations in reflectance, two correction methods were applied. C-correction was implemented to adjust for illumination differences caused by varying slopes and aspects, accounting for topographic shading effects and ensuring more consistent reflectance values across different terrain conditions [18]. Additionally, slope-matching correction was used to normalize reflectance values by adjusting for solar zenith and azimuth angles using a digital elevation model (DEM) [19, 20]. This approach reduced distortions from slope-induced variations in reflectance, improving the comparability of NDVI values across different terrains.

NDVI measures vegetation greenness by leveraging spectral reflectance values obtained from satellite imagery in the red and near-infrared (NIR) regions of the electromagnetic spectrum [21]. Similar to EVI, NDVI values range from -1 to 1, with higher values generally indicating healthier, denser vegetation. The contrast between the high NIR reflectance of healthy vegetation and the lower NIR reflectance (and higher red reflectance) of non-vegetative surfaces forms the basis of this index.

While NDVI is widely used for its simplicity and robustness in capturing broad-scale vegetation dynamics, it is sensitive to atmospheric conditions and soil background effects, which can

occasionally impact measurement accuracy. Despite these limitations, NDVI remains a valuable tool for assessing vegetation health and recovery due to its extensive historical application and proven effectiveness in long-term monitoring [22, 23].

NDVI was chosen over the EVI for this section due to its stability in capturing long-term vegetation trend dynamics. Unlike EVI, which enhances sensitivity to subtle vegetation changes by minimizing atmospheric and soil background influences [22], NDVI provides a more consistent representation of broad-scale vegetation trends [24]. Given this section's objective of assessing long-term vegetation recovery trends rather than capturing short-term fluctuations, NDVI was deemed the more appropriate metric for time-series analysis.

NDVI was calculated for each Landsat image using the following equation:

$$\mathrm{NDVI} = \frac{(\mathrm{NIR} - \mathrm{RED})}{(\mathrm{NIR} + \mathrm{RED})},$$

where NIR corresponds to SR Band 5 for Landsat 5 and 7 or Band 4 for Landsat 8 and 9, while RED corresponds to SR Band 4 for Landsat 5 and 7 or Band 3 for Landsat 8 and 9.

To assess vegetation trends over time, NDVI values were aggregated annually by computing the median NDVI for each year using GEE. The time series was divided into three distinct periods: Before Landslide, After Landslide, and After Drone Intervention. The annual median NDVI values for each period were extracted, and a line graph was generated in R (ggplot2) to visualize NDVI trends, with shaded background colors representing each phase.

2.2.2. Sentinel-2-based Enhanced Vegetation Index analyses

Sentinel-2 Harmonized SR imagery from the Copernicus Sentinel-2 mission was accessed via GEE to assess vegetation health changes across the three treatment areas and the Control Area. The imagery was filtered to retain only images with less than 20% cloud cover, and cloud-contaminated pixels were masked using the QA60 band. To ensure a consistent and balanced assessment of vegetation health changes, equal time periods were defined for pre- and post-intervention comparisons. The pre-intervention period spanned from August 2016 to May 2019 (33 months), while the post-intervention period covered from August 2019 to May 2022 (also 33 months). The three months during which the revegetation project took place (May 2019 to July 2019) were excluded from both periods.

Unlike Landsat imagery, Sentinel-2 data are more temporally limited, particularly in regions with frequent cloud cover, such as Taiwan. Therefore, restricting the analysis to specific seasons would significantly reduce the number of available observations, potentially compromising the study's robustness. Therefore, to maximize data availability while maintaining consistency in temporal comparisons, imagery was included from all months rather than being constrained to a specific seasonal window. This consideration is taken into account when identifying patterns and making comparisons, ensuring that any observed changes in vegetation health are interpreted within the context of potential seasonal influences.

To minimize the impact of terrain on vegetation reflectance, a slope-matching topographic correction method was applied. Using the Shuttle Radar Topography Mission (SRTM) DEM, slope and aspect were computed for each image, and solar zenith and azimuth angles were incorporated to normalize reflectance values. This correction ensured that observed vegetation changes were attributed to actual vegetation recovery rather than variations in terrain-induced illumination. Areas where the correction was invalid, such as those where relative illumination conditions resulted in negative or near-zero cosine values, were masked to maintain data integrity.

Additionally, EVI was calculated using Sentinel-2 Harmonized imagery. EVI was selected over NDVI for this section due to its improved sensitivity to subtle variations in vegetation conditions, particularly in areas of high biomass. Unlike NDVI, which can become saturated in dense vegetation, EVI incorporates additional corrections for atmospheric effects and canopy background signals, making it more suitable for detecting small-scale vegetation changes while minimizing distortions caused by soil brightness [22]. This enhanced sensitivity enables a more precise comparison of vegetation health changes in response to the intervention.

EVI was calculated using the standard formula in GEE:

$$\mathrm{EVI} = 2.5 \times \frac{\mathrm{NIR} - \mathrm{RED}}{(1 + \mathrm{NIR} + 6 \times \mathrm{RED} - 7.5 \times \mathrm{BLUE})},$$

where Band 5 (Landsat 5 and 7) or Band 4 (Landsat 8 and 9) corresponds to the NIR region, Band 4 (Landsat 5 and 7) or Band 3 (Landsat 8 and 9) corresponds to the red region, and Band 2 (Landsat 5, 7, 8, and 9) corresponds to the blue region of the electromagnetic spectrum. This formulation enhances the sensitivity of the index while minimizing the effects of atmospheric conditions. This equation follows a similar approach to Zeng et al. [25].

With all necessary corrections applied to the Sentinel-2 collection and the completion of EVI calculations, the following analyses were conducted to assess vegetation changes in response to drone revegetation efforts. These analyses included pre- and post-treatment spatial changes, ECDFs, PDFs, and a K-S test. By incorporating these statistical techniques, we aimed to capture both immediate and sustained vegetation recovery trends, ensuring a comprehensive evaluation of the intervention's impact.

Pre- and post-treatment spatial changes

For each study and Control Area, median composite images were generated for both the pre- and post-intervention periods by calculating the median EVI value for each pixel across all available images within the respective time frames. These composite images were then clipped to the study area boundaries. Difference images were created by subtracting the pre-intervention median EVI from the post-intervention median EVI to highlight spatial variations in vegetation change.

The final EVI maps were color-coded to visually depict vegetation health dynamics. Pre- and post-intervention maps used an EVI scale ranging from 0 to 0.8, where brown tones represented low vegetation health and green tones indicated high vegetation health. Difference maps were scaled from −0.25 to 0.25, where negative values (brown) indicated vegetation loss, positive values (green) signified vegetation recovery, and white areas represented minimal change. These visualizations provided a spatial assessment of vegetation responses across the treated and control areas, offering insights into the intervention's impact on vegetation health over time.

Empirical cumulative distribution function analysis

ECDFs were used to evaluate distributional changes in EVI values between pre- and post-intervention periods. This nonparametric approach provides insights into shifts across the entire vegetation health spectrum rather than relying solely on mean or median values.

A post-intervention ECDF positioned below the pre-intervention ECDF at a given EVI value indicates improved vegetation conditions, whereas a post-intervention ECDF positioned above suggests potential vegetation decline. This method allows for a more nuanced assessment of effectiveness by capturing vegetation health changes across different EVI levels.

A shift in the post-intervention ECDF relative to the pre-intervention ECDF provides insight into distributional changes in vegetation health. When the post-intervention ECDF is positioned below the pre-intervention ECDF at a given EVI value, it indicates that a greater proportion of areas exhibited EVI values exceeding that threshold post-intervention, suggesting overall vegetation improvement. Conversely, when the post-intervention ECDF is positioned above the pre-intervention ECDF, it signifies that a larger share of areas had EVI values at or below that level post-intervention, indicating a potential decline in vegetation health.

By analyzing the full ECDF curves, we assessed whether the intervention led to an overall increase or decrease in vegetation health and determined whether these changes were concentrated within specific EVI ranges. This approach allowed for a more detailed understanding of vegetation condition trends across the study areas beyond simple mean or median comparisons.

Probability density function analysis

To assess changes in vegetation health over time, PDFs of EVI values were computed for both the pre- and post-intervention periods utilizing the pre-processed Sentinel-2 collection. PDFs provide a smooth representation of EVI distributions, allowing for the visualization of shifts in vegetation health and detecting whether the intervention resulted in a higher density of areas with increased vegetation greenness.

Kernel density estimates were generated in R using the density() function, which applies to a Gaussian kernel to estimate the probability density across the range of EVI values. This nonparametric approach captures the underlying distribution of vegetation health without assuming a predefined statistical model. The pre- and post-intervention PDFs were computed separately to evaluate differences in the distribution of EVI values before and after the intervention. The density estimates for both periods were converted into data frames to streamline visualization and comparison using the ggplot2 library in R.

By examining changes in the shape and position of the PDFs, we can identify shifts in vegetation health across the study areas. For example, an increase in the density of higher EVI values in the post-intervention period would suggest improved vegetation conditions, whereas a shift toward lower EVI values may indicate potential declines in vegetation health. This approach provides a more detailed understanding of vegetation recovery by analyzing distributional changes rather than relying solely on summary statistics, such as mean or median EVI values.

Kolmogorov–Smirnov test

To statistically evaluate changes in EVI values before and after the intervention, we conducted a K-S test, a nonparametric method that compares the empirical distribution functions (EDFs) of two datasets. This test is particularly well suited for detecting distributional shifts as it does not assume a specific underlying distribution and is robust to differences in data scale [26].

The analysis was performed in R, leveraging its comprehensive statistical packages. First, pre- and post-treatment EVI data were imported from comma-separated values (CSV) files and structured using the tidyverse suite for data manipulation. The K-S test was then applied to each study area, comparing pre- and post-intervention EVI distributions to assess whether significant differences existed.

The null hypothesis (H_0) assumes that the pre- and post-intervention EVI distributions are identical, while the alternative hypothesis (H_1) suggests that a statistically significant shift occurred due to the intervention. The test statistic measures the maximum difference between the EDFs of the two datasets, and a low p-value ($p < 0.05$) indicates a significant change in vegetation health distribution.

This approach provides a quantitative measure of the intervention's impact, complementing visual interpretations from ECDF and PDF analyses. By identifying shifts across the entire EVI distribution, the K-S test offers a rigorous assessment of whether the observed vegetation changes were statistically meaningful.

Long-term pre- and post-intervention analysis

Lastly, to assess a long-term revegetation trends at high spatial resolution, Sentinel-2 imagery was analyzed over a multiyear period (2017–2024). To evaluate changes in vegetation health following the intervention, the time series was divided into two time periods: pre-treatment (2017–2019) and post-treatment (August 2019–2024).

The year 2017 was chosen as the start of the pre-intervention period since July 2017 was the earliest date for which Sentinel-2 imagery was available for our study areas. The median EVI was calculated for each study area at a 10-m resolution, and an EVI time series was generated using a mean reducer across the extent of each study area. This temporal assessment leveraged the high-resolution capabilities of Sentinel-2 data to capture vegetation dynamics more effectively over time.

This time series of EVI values provided a detailed evaluation of vegetation changes over time, enabling a more comprehensive analysis of the revegetation process, particularly in assessing the effectiveness of drone-assisted interventions.

To compare vegetation conditions between pre- and post-treatment periods, scatter plots of EVI values over time were generated in R (ggplot2). Each point in the scatter plot represented an EVI value recorded on a specific date, allowing for a clear visualization of temporal trends. A linear model trend line was fitted separately for the pre- and post-treatment periods to illustrate directional changes in vegetation health. The overall median EVI value for the entire period, spanning both pre- and post-intervention time frames, was indicated using a horizontal reference line. To enhance interpretability, color mapping was applied to visually distinguish vegetation variations over time. This visualization approach facilitated an intuitive assessment of vegetation dynamics, providing insights into the spatial and temporal effectiveness of the intervention across different study areas. By integrating high-resolution spatial data with a

long-term temporal analysis, this method enabled a robust evaluation of vegetation recovery trends, offering valuable information on the impact of drone-assisted revegetation.

3. Results

3.1. Long-term Landsat Normalized Difference Vegetation Index

The NDVI time series shown in **Figure 2** for Study Area 1 highlights distinct vegetation trends across three periods: Before Landslide (2000–2012), After Landslide (2012–2019), and After Drone Intervention (2019–2024). Before 2012, NDVI values remained stable, consistently above 0.7, indicating healthy vegetation. A temporary dip in 2006 suggests a short-lived disturbance, but recovery was swift. Following the 2012 landslide, NDVI declined, reaching its lowest point in 2014 (below 0.65), reflecting a negative change in vegetation loss. The post-landslide period was characterized by high variability, with occasional signs of regrowth but no full return to pre-landslide levels, suggesting slow and inconsistent natural recovery.

From 2019 onward, after the drone intervention, NDVI showed a steady upward trend, approaching 0.8 by 2022–2024, comparable to pre-landslide conditions. These results indicate that while natural regeneration was slow and inconsistent, intervention efforts played a key role in accelerating recovery.

The NDVI time series shown in **Figure 2** for Study Area 2 follows three phases: Before Landslide (2000–2004), After Landslide (2004–2019), and After Drone Intervention (2019–2024). Before 2004, NDVI remained above 0.65, reflecting a stable ecosystem. The landslide caused a sharp drop to 0.3, marking a significant vegetation loss. Post-landslide recovery was slow and uneven, with NDVI fluctuating between 0.5 and 0.6 for almost a decade, indicating inconsistent natural regrowth. However, a more stable upward trend began in 2014, with NDVI surpassing 0.7 by 2018–2019.

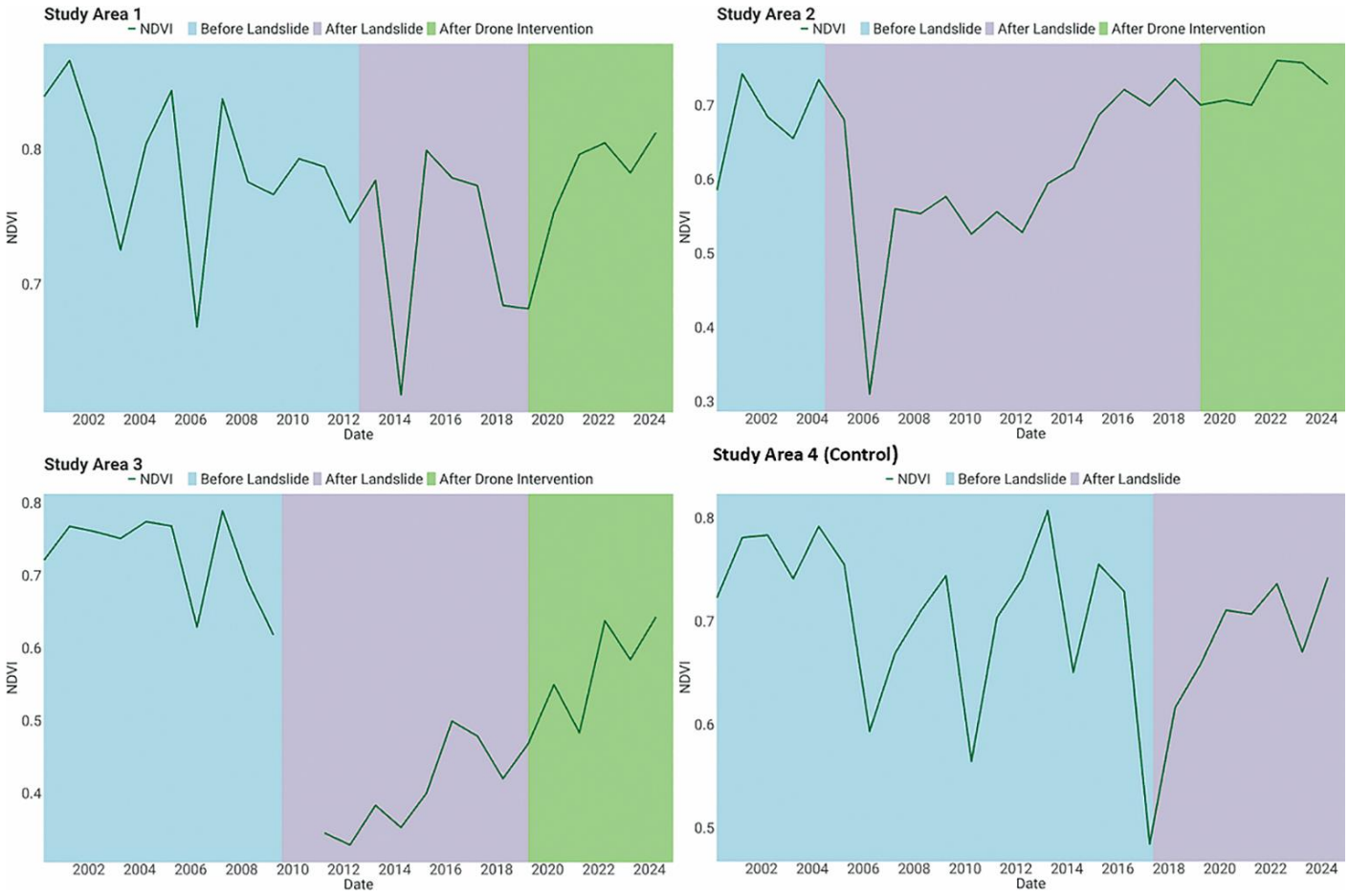

Figure 2 • Normalized Difference Vegetation Index (NDVI) time series for Study Areas 1–3 and the Control Area from 2000 to 2024, illustrating vegetation trends before and after landslide events, as well as post-drone intervention recovery. Each time series is divided into three distinct periods: Before Landslide (blue), After Landslide (purple), and After Drone Intervention (green). In all study areas, NDVI declines sharply following landslide events, with varying degrees of recovery. Study Area 1 exhibits slow and inconsistent natural recovery before showing a noticeable increase after 2019, coinciding with drone-assisted restoration. Study Area 2 shows a different pattern, with significant NDVI improvements beginning around 2016, making it unclear whether the recovery was due to natural revegetation or drone intervention. The Control Area, which experienced a landslide in 2017, shows a rapid recovery compared to the study areas, suggesting that factors such as terrain stability and environmental conditions influenced post-landslide regrowth. Overall, the results highlight the impact of landslides on vegetation loss and the potential role of drone-based interventions in accelerating ecosystem recovery.

After 2019, coinciding with the drone intervention, NDVI showed a sustained increase, remaining above 0.7 through 2024. While this suggests successful revegetation efforts, the steady recovery trend beginning in 2016 implies that a combination of natural regrowth, environmental factors, and potential land management contributed to vegetation restoration.

For Study Area 3, the NDVI time series shown in **Figure 2** follows the same pattern: Before Landslide (2000–2009), After Landslide (2009–2019), and After Drone Intervention (2019–2024). Before 2009, NDVI values were stable (>0.7), apart from minor fluctuations. The 2009 landslide caused an immediate NDVI drop below 0.3, exposing bare soil and disrupting vegetation. No data were available for 2010 due to persistent cloud cover from the same weather system. Recovery between 2012 and 2018 was slow and inconsistent, with NDVI fluctuating between 0.3 and 0.5, likely due to soil degradation and erosion. However, after 2019, NDVI displayed a consistent upward trajectory, reaching 0.6 by 2022 and continuing toward pre-landslide levels. While some vegetation improvement was visible before the intervention, the sharper post-2019 increase suggests a positive effect of targeted restoration efforts.

For the Control Area, shown in **Figure 2**, NDVI remained high (0.7–0.8) before 2017, with occasional fluctuations likely due to seasonal droughts and climate variability. Following the 2017 landslide, NDVI dropped below 0.5 in 2018, indicating substantial vegetation loss. Unlike the other study areas, the control site recovered quickly, surpassing 0.7 by 2020 and maintaining pre-landslide levels through 2024.

3.2. Pre- and post-treatment spatial changes

The pre-treatment, post-treatment, and difference maps for Study Area 1, shown in **Figure 3**, indicate positive vegetation health changes following the intervention. The pre-treatment map displays moderate to high EVI values across most of the area, with some lower vegetation health patches, particularly on the east boundary, suggesting degraded or bare land. Post-treatment, overall vegetation health improved, with a reduction in low-EVI areas, although some patches of lower vegetation health persist in the same regions.

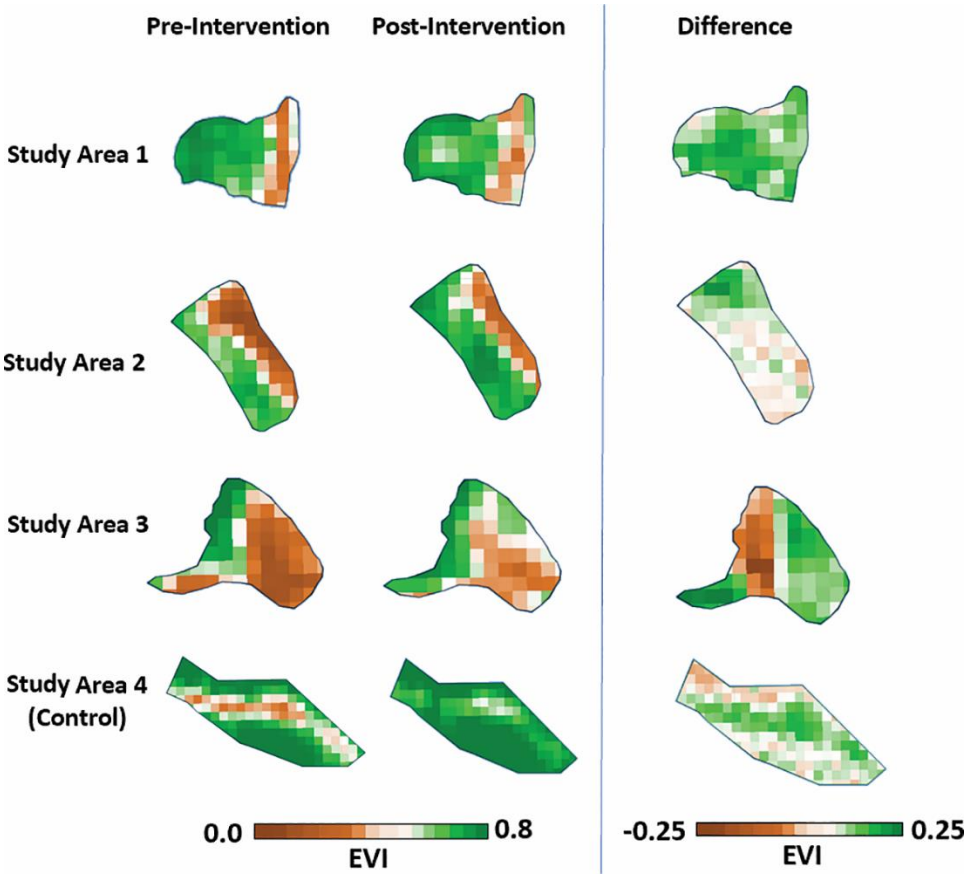

Figure 3 • Spatial distribution of Enhanced Vegetation Index (EVI) values across study areas before and after the revegetation intervention, along with vegetation change (difference) maps. The first column represents pre-treatment EVI values, where green areas indicate higher vegetation health and brown areas signify lower vegetation health or bare land. The second column shows post-treatment EVI values, revealing changes following the intervention, while the third column presents the difference maps, highlighting the net change in EVI values between the pre- and post-treatment periods. Study Area 1 shows a notable improvement in vegetation health, with a visible reduction in brown areas and an increase in green shades. The difference maps confirm a net positive change in most regions, though some areas remain unchanged (white) or show minimal degradation. In Study Area 2, vegetation gains are primarily concentrated in the upper portion, while the rest of the area remains largely unchanged or experiences minor losses. Study Area 3 exhibits strong recovery in many regions, as indicated by large green patches in the difference map. However, some areas continue to show degradation (brown patches), suggesting that the response to the intervention has been spatially variable. Study Area 4 (Control), where no intervention was applied, shows moderate changes over time, with a mix of positive and negative changes. This suggests that some vegetation fluctuations may be due to natural variations, but the stronger improvements in treated areas indicate that the intervention played a role in recovery.

The difference map provides a clearer picture of these variations, showing a dominance of green shades, which indicates a net positive change in EVI values and suggests successful vegetation recovery (**Figure 3**). The reduction in brown areas further confirms that previously degraded regions benefited from the intervention. White areas in the difference map indicate minimal change, reflecting stable vegetation conditions (**Figure 3**). Overall, the results suggest that the intervention had a positive impact on vegetation health, with most of the study area experiencing an increase in EVI values.

The pre-treatment map for Study Area 2, shown in **Figure 3**, reveals widespread low vegetation health, especially along the upper and eastern boundaries, while some areas along the western border exhibit moderate to high EVI values. Post-treatment, a noticeable improvement in vegetation health is observed, with a reduction in low-EVI areas and an expansion of green regions, particularly in the upper and central portions of the study area. However, some regions along the right border remain degraded (**Figure 3**).

The difference map highlights the magnitude and direction of vegetation change, with some light green and predominantly white shades indicating minimal changes in vegetation health. The persistence of brown patches in certain areas suggests ongoing vegetation stress or degradation despite overall improvements. These findings indicate a moderate improvement in vegetation health, with the intervention contributing to recovery, though some areas remain resistant to change.

Study Area 3 exhibits a complex pattern of vegetation change over time, as shown in **Figure 3**. The pre-treatment map shows heterogeneous vegetation conditions, with low EVI values concentrated in the central and lower-eastern sections, while the northern and southwestern portions display moderate to high vegetation health. Post-treatment, the response to the intervention varies. While some regions, particularly in the lower-western section, show visible improvement, other areas, including parts of the central and southeastern sections, remain degraded or exhibit continued stress.

The difference map confirms this spatial variation, with green areas indicating vegetation recovery, while brown areas signify a continued decline in EVI values (**Figure 3**). White areas represent minimal change. Overall, the results suggest that while the intervention had some positive effects, certain regions remained unchanged or continued to degrade.

The Control Area provides a baseline for comparison in the absence of intervention. The pre-treatment map displayed in **Figure 3** shows moderate to high vegetation health, with some localized brown patches, indicating areas of vegetation stress or degradation. Post-treatment, vegetation health improves naturally, with previously degraded areas transitioning to green, suggesting a gradual recovery over time. The difference map highlights this natural trajectory, with light green and white areas dominating, suggesting that most of the Control Area either remained stable or experienced slight improvements. Some brown patches persist, particularly in the upper-left section, indicating localized vegetation decline.

3.3. Enhanced Vegetation Index empirical cumulative distribution functions

The ECDF comparison for Study Area 1, shown in **Figure 4**, reveals mixed effects of the intervention on vegetation health. The post-intervention ECDF lies below the pre-intervention ECDF at lower EVI values, indicating that fewer areas had very low EVI values after the intervention, suggesting an overall improvement in degraded areas. This is further supported by an increase in median EVI from 0.3 to 0.36 post-intervention. However, at EVI values above 0.35, the post-intervention ECDF rises above the pre-intervention ECDF, indicating that fewer areas retain moderate to high vegetation health compared to pre-intervention conditions. This suggests that while the intervention was beneficial for the most degraded regions, it coincided with a decline in vegetation health in previously stable areas. Overall, these results indicate that the intervention had both positive and negative effects, improving conditions in severely degraded pixels while reducing vegetation health in areas that initially had moderate EVI values.

The ECDF comparison for Study Area 2, shown in **Figure 4**, suggests a decline in vegetation health following the intervention. The post-intervention ECDF is above the pre-intervention ECDF at lower EVI values, indicating an increase in low-EVI areas. This is further supported by a drop in median EVI from 0.21 pre-intervention to 0.14 post-intervention, suggesting a general shift toward lower vegetation health. In the moderate EVI range (0.2–0.6), the post-intervention ECDF remains above the pre-intervention ECDF, meaning that many areas with previously moderate vegetation health shifted toward lower values. At higher EVI values (above 0.6), the ECDF curves for pre- and post-intervention converge, suggesting that regions with already high vegetation health remained stable. Overall, these results indicate a general reduction in vegetation health, particularly in areas that previously had moderate EVI values, while the healthiest regions were largely unaffected.

The ECDF comparison for Study Area 3 in **Figure 4** shows a notable shift in vegetation health between the pre- and post-intervention periods. The post-intervention ECDF (dark green) is consistently below the pre-intervention ECDF (light brown), particularly at lower EVI values, indicating an overall increase in vegetation health. The median EVI has shifted from approximately 0.21 to 0.3, suggesting a meaningful improvement in vegetation conditions following the intervention. At lower EVI values, the post-intervention curve rises more gradually compared to the pre-intervention curve, implying a reduction in the proportion of degraded areas. Conversely, at higher EVI values, the curves remain close, indicating that healthier regions have remained stable. This pattern suggests that the intervention had a positive impact on vegetation health, with a general shift toward higher EVI values and an improvement in median vegetation condition.

The ECDF comparison for the Control Area shown in **Figure 4** suggests a slight decline in vegetation health between the pre- and post-intervention periods. The median EVI decreased from 0.35 (pre-intervention) to 0.31 (post-intervention), indicating a shift toward lower vegetation health. At lower EVI values, the post-intervention ECDF (dark green) is slightly above the pre-intervention ECDF (light brown), suggesting a small increase in degraded areas. This implies that more areas have shifted to lower vegetation index values post-intervention. In the moderate EVI range (0.2–0.4), the post-intervention curve remains above the pre-intervention curve, reinforcing the trend of declining vegetation health. At higher EVI values (above 0.4), the curves converge, indicating that regions with already high vegetation health remained relatively stable. Overall, the results indicate a slight degradation in vegetation conditions within the Control Area, as reflected in the downward shift in median EVI and the increased proportion of lower EVI values post-intervention.

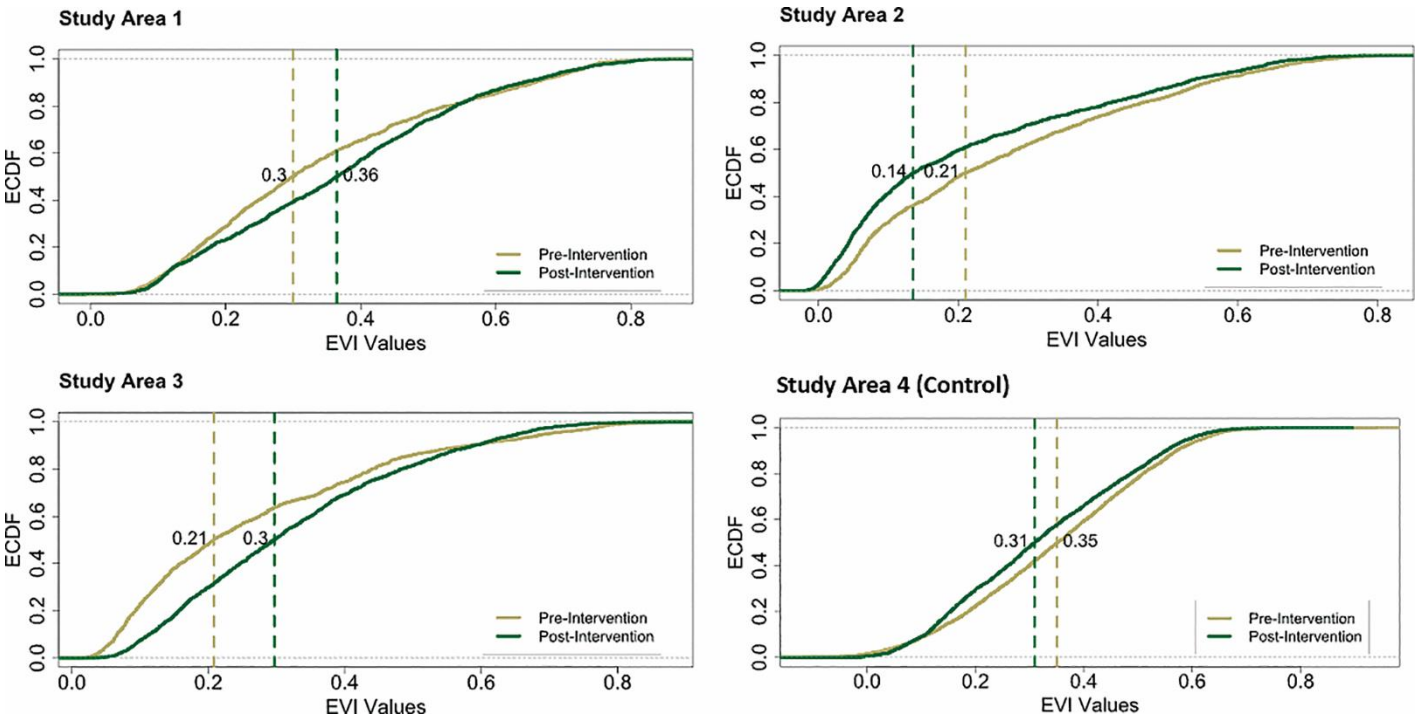

Figure 4 • Empirical cumulative distribution functions (ECDFs) comparing vegetation health, as measured by Enhanced Vegetation Index (EVI) values, before (pre-intervention) and after (post-intervention) the intervention across Study Areas 1–3 and the Control Area. In Study Area 1, the post-intervention ECDF indicates an improvement in vegetation health, as the median EVI has increased from 0.30 to 0.36. The post-intervention ECDF lies below the pre-intervention ECDF at lower EVI values, meaning that fewer areas have poor vegetation health, while higher EVI values remain stable. In Study Area 2, the post-intervention ECDF shows a significant upward shift at lower and moderate EVI values, highlighting a general reduction in vegetation health following the intervention, along with a significant decrease in the median EVI, with little change in the highest EVI values. In Study Area 3, the post-intervention ECDF shows a rightward shift in vegetation health, with the median EVI increasing from 0.21 to 0.30. The post-intervention ECDF lies below the pre-intervention ECDF at lower EVI values, indicating that fewer areas have poor vegetation health. This suggests an overall improvement in vegetation conditions rather than stability. In the Control Area, there is a slight decline in vegetation health, as indicated by a decrease in the median EVI from 0.35 to 0.31. The post-intervention ECDF lies above the pre-intervention ECDF at lower EVI values, meaning that a greater proportion of areas now have lower EVI values. However, the ECDFs for higher EVI values remain nearly identical, suggesting that the healthiest areas remained stable despite the overall decline.

3.4. Enhanced Vegetation Index probability density functions

The PDF for Study Area 1 shown in **Figure 5** indicates positive vegetation health changes following the intervention. At lower EVI values, the post-intervention distribution (green curve) is below the pre-intervention distribution, indicating a reduction in degraded areas. In the medium EVI range, the post-intervention curve rises above the pre-intervention curve, suggesting that a portion of the study area shifted from low to moderate vegetation health. The peaks of the distributions support this trend, with the post-intervention peak occurring at a higher EVI value than the pre-intervention peak. This is further confirmed by the increase in median EVI, which rose from 0.22 to 0.35 post-intervention. However, at higher EVI values, the post-intervention curve falls slightly below the pre-intervention curve, indicating a decline in vegetation health in areas that initially had the highest EVI values. This suggests that the intervention benefited lower EVI regions but may have contributed to some loss in areas that previously had the strongest vegetation cover.

The PDF for Study Area 2 shown in **Figure 5** indicates a decline in vegetation health post-intervention. The post-intervention curve is above the pre-intervention curve at lower EVI values, reflecting an increment in degraded areas. In the moderate EVI range, the post-intervention curve falls below the pre-intervention curve, suggesting that some areas previously classified as moderate vegetation shifted toward lower EVI values. The peaks of the curves reinforce this trend, with the post-intervention peak occurring at a slightly lower EVI value than before. This is further supported by the decline in median EVI, indicating a general downward shift in vegetation health. At higher EVI values, the post-intervention curve remains below the pre-intervention curve, suggesting a slight decrease in the proportion of areas with high vegetation health. These outcomes suggest that the intervention was not effective in improving vegetation health in the short term for Study Area 2, leading to a slight overall decline across areas with initially moderate to high vegetation health.

The PDF comparison for Study Area 3 in **Figure 5** shows an overall increase in observed values post-intervention. The post-intervention curve is above the pre-intervention curve at higher values, reflecting a positive shift in the distribution. In the lower value range, the post-intervention curve falls below the pre-intervention curve, suggesting that some areas previously concentrated at smaller values have shifted upward. The peaks of the curves reinforce this trend, with the post-intervention peak occurring at a slightly higher value than before. This is further supported by the increase in the median value, indicating a

general upward shift. These outcomes suggest that the intervention was associated with an overall increase in values across Study Area 3, resulting in a broader distribution and an upward shift in overall vegetation health.

The PDF for the Control Area in **Figure 5** indicates a negative shift in the distribution of vegetation health values over time. The post-period distribution (green) exhibits a higher density at lower values compared to the pre-period distribution (yellow), suggesting an increase in the proportion of areas experiencing vegetation decline. In the moderate range, the post-period curve initially rises above the pre-period curve but then subsequently falls below it, indicating that while some areas retained moderate vegetation health, others transitioned to lower values. The peaks oof the distributions further support this trend, with the post-period peak occurring at a slightly lower value than before, reflecting an overall downward shift. Additionally, the decline in the median value reinforces this pattern, suggesting a general reduction in vegetation health across the area. At the higher end of the distribution, the post-period curve remains below the pre-period curve, indicating a decrease in the proportion of areas maintaining strong vegetation health. These findings suggest that, in the absence of intervention, vegetation health in the Control Area exhibited a short-term downward trend.

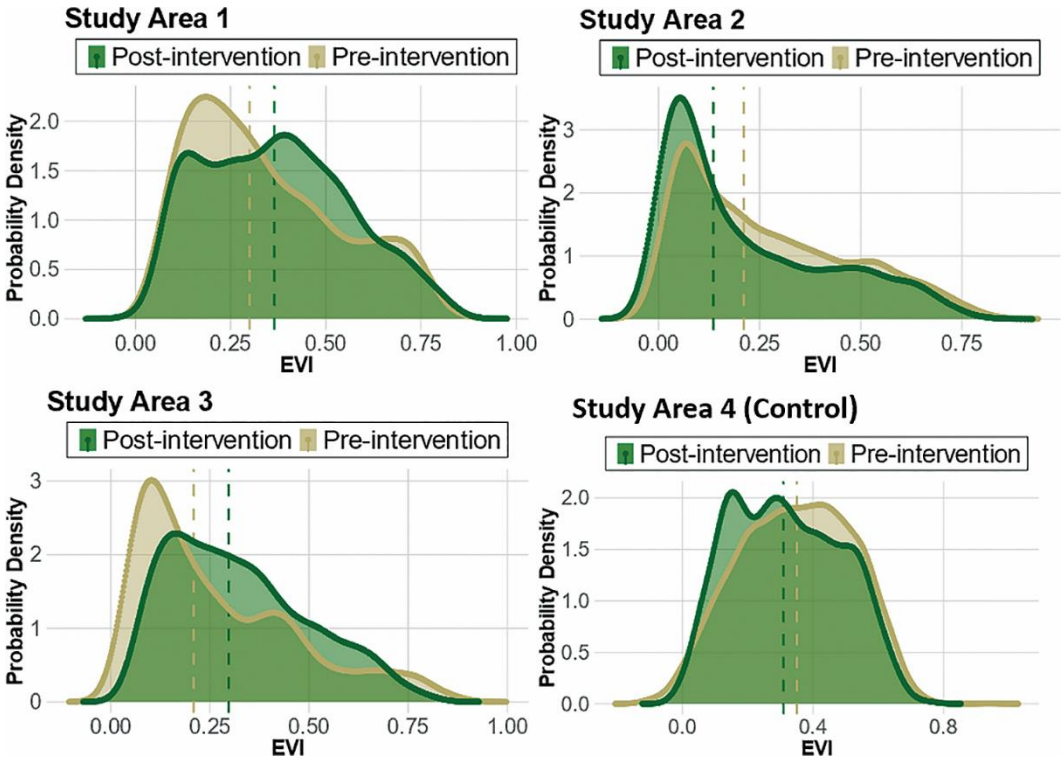

Figure 5 • The probability density functions illustrate changes in vegetation health before and after the intervention across the three study areas and the Control Area. In Study Area 1, the post-intervention distribution (green) shows a reduction in the proportion of areas with low vegetation health and an increase in medium Enhanced Vegetation Index (EVI) values, along with a rise in the median EVI, indicating an overall improvement. Study Area 2 exhibits an increase in low EVI values post-intervention, suggesting a decline in vegetation health in some areas and a slight decrease in the median EVI. In Study Area 3, vegetation health appears to have improved post-intervention, as indicated by a slight upward shift in the median EVI and an increase in the proportion of areas with higher EVI values. While some regions still exhibit lower EVI, the overall distribution suggests enhanced vegetation conditions compared to pre-intervention levels. The Control Area, where no intervention was implemented, shows a significant decline in vegetation health, with a shift toward lower EVI values and a substantial decrease in the median EVI, suggesting that in the absence of intervention, vegetation health deteriorated over time.

3.5. Kolmogorov–Smirnov tests

The two-sample K-S test results in **Table 2** statistically confirm shifts in EVI distributions between the pre- and post-intervention periods across all study areas. The null hypothesis (H_0) of the K-S test posited no difference between the distributions, but the test results revealed statistically significant changes ($p < 0.05$) in all four locations, affirming notable shifts in vegetation health.

Study Area 1 exhibited a moderate but meaningful shift ($D = 0.13$), accompanied by an increase in mean EVI from 0.34 to 0.37. This result suggests that the drone-facilitated revegetation had a positive impact on vegetation health, as both the statistical test and the observed EVI increase indicate a shift toward improved conditions. Similarly, Study Area 3 demonstrated the most substantial shift among the intervention sites ($D = 0.2018$), with mean EVI rising from 0.27 to 0.31.

Conversely, Study Area 2 exhibited a negative shift, with the K-S test statistic ($D = 0.158$) indicating a substantial departure from the pre-intervention distribution in the opposite direction. The mean EVI in this area decreased from 0.27 to 0.20, suggesting that seeding efforts were less effective in promoting vegetation recovery. The downward trend in vegetation health in this area, as confirmed by both the EVI decline and K-S test, highlights the variability in revegetation success across different conditions. The control site exhibited the smallest test statistic ($D = 0.08$) but still showed a statistically significant shift. The mean EVI

declined slightly from 0.34 to 0.32, suggesting that natural regrowth was insufficient to restore vegetation cover in the short term. While some degree of vegetation change was observed, the smaller magnitude of the shift compared to the intervention sites reinforces the notion that active revegetation efforts contributed more substantially to improvements in vegetation health.

3.6. Long-term pre- and post-intervention analysis

For Study Area 1, as shown in **Figure 6**, the pre-treatment period is characterized by lower EVI values and a sustained declining trend, indicating sparse vegetation cover before to the intervention. Throughout this period, a larger proportion of EVI values consistently fluctuated below the median reference line, reinforcing the pattern of limited vegetation presence. Following the intervention in May, June, and August 2019, a noticeable shift in EVI distribution emerges, marked by an increasing presence of green-colored points, suggesting improvements in vegetation health. Unlike the pre-treatment period, the post-intervention trend line exhibits a positive trajectory, indicating a steady increase in vegetation cover over time. This upward trend suggests that the intervention contributed to sustained improvements in vegetation health. However, despite the overall positive trend, variability in EVI values remains, highlighting a heterogeneous recovery process. While some areas demonstrate significant regrowth, others exhibit slower recovery, suggesting that external factors may still influence the extent and consistency of vegetation recovery across Study Area 1.

For Study Area 2, as shown in **Figure 4**, the pre-treatment period is characterized by lower EVI values and a gradual decreasing trend, indicating limited and inconsistent vegetation cover before the intervention. Following the intervention in May, June, and August 2019, there is no clear upward shift in EVI distribution, with values continuing to exhibit significant seasonal variability. Unlike Study Area 1, the post-intervention trend line does not demonstrate a sustained positive trajectory in magnitude, suggesting that vegetation recovery was limited. Instead, EVI values remain highly variable, with periods of increased vegetation followed by subsequent declines. This pattern suggests that while certain areas may have experienced temporary improvements in vegetation health, overall recovery remained inconsistent.

For Study Area 3, as shown in **Figure 5**, the pre-treatment period is characterized by lower EVI values with a declining trend, indicating sparse vegetation cover before the intervention. During this period, most EVI values fluctuate below the median reference line, reinforcing the pattern of limited vegetation presence. Following the intervention in May, June, and August 2019, a noticeable shift in EVI distribution emerges, with an increasing number of green-colored points, suggesting improvements in vegetation health. Unlike Study Area 2, the post-intervention trend line in Study Area 3 exhibits a positive trajectory, indicating a gradual but sustained increase in vegetation cover over time. While EVI values continue to display some variability, the overall upward trend suggests that revegetation efforts had a measurable impact on vegetation recovery. However, the persistence of fluctuations in EVI values highlights a heterogeneous recovery process, where some areas demonstrate significant regrowth, while others recover at a slower pace.

Table 2 • Summary statistics comparing pre- and post-intervention Enhanced Vegetation Index values across study sites in a revegetation project

Study area number	Area's number of pixels	Sample size (months)	Number of pre-intervention images	Number of post-intervention images	Pre-intervention EVI (μ)	Post-intervention EVI (μ)	μ Change	K-S test D	p-Value
1	53	33	33	44	0.34	0.37	0.03	0.13	1.613×10^{-10}
2	68	33	37	56	0.27	0.20	-0.04	0.15	2.2×10^{-16}
3	60	33	37	56	0.27	0.31	0.05	0.20	2.2×10^{-16}
4 (Control)	152	33	32	44	0.34	0.32	-0.03	0.08	4.815×10^{-12}

The table presents the number of pixels analyzed per site, sample size (in months), and the number of images available in the before- and after-intervention periods. Furthermore, it includes the mean Enhanced Vegetation Index (EVI) values pre- and post-intervention, the change in mean EVI (μ change), and results from the Kolmogorov–Smirnov (K-S) test assessing distributional shifts. Lastly, the p-values for the K-S test are included, indicating whether or not observed changes are statistically significant. Overall, Study Areas 1 and 3 showed increments in mean EVI (from 0.34 to 0.37 and from 0.27 to 0.31, respectively), suggesting a positive effect from the intervention. Study Area 2, however, experienced a decline in EVI (from 0.27 to 0.20), indicating potential challenges in vegetation recovery. The control site showed a slight decrease in EVI values (from 0.34 to 0.32), suggesting that natural recovery was ineffective in restoring vegetation cover in the short term for the Control Area. All changes were statistically significant ($p < 0.05$), with the K-S test confirming notable shifts in EVI distributions across intervention sites. Study Areas 1–3 exhibited K-S test statistics of 0.13, 0.158, and 0.2018, respectively, indicating varying degrees of divergence between pre- and post-intervention EVI distributions. The largest shift occurred in Study Area 3 ($D = 0.2018$), suggesting a substantial change in vegetation cover following the intervention. Study Area 2 ($D = 0.158$) also showed considerable change but in the opposite direction, as EVI decreased post-intervention. Study Area 1 ($D = 0.13$) displayed a moderate yet significant shift, corresponding to a positive EVI change. The control site had the smallest K-S statistic ($D = 0.08$), reflecting minimal distributional change in the absence of intervention.

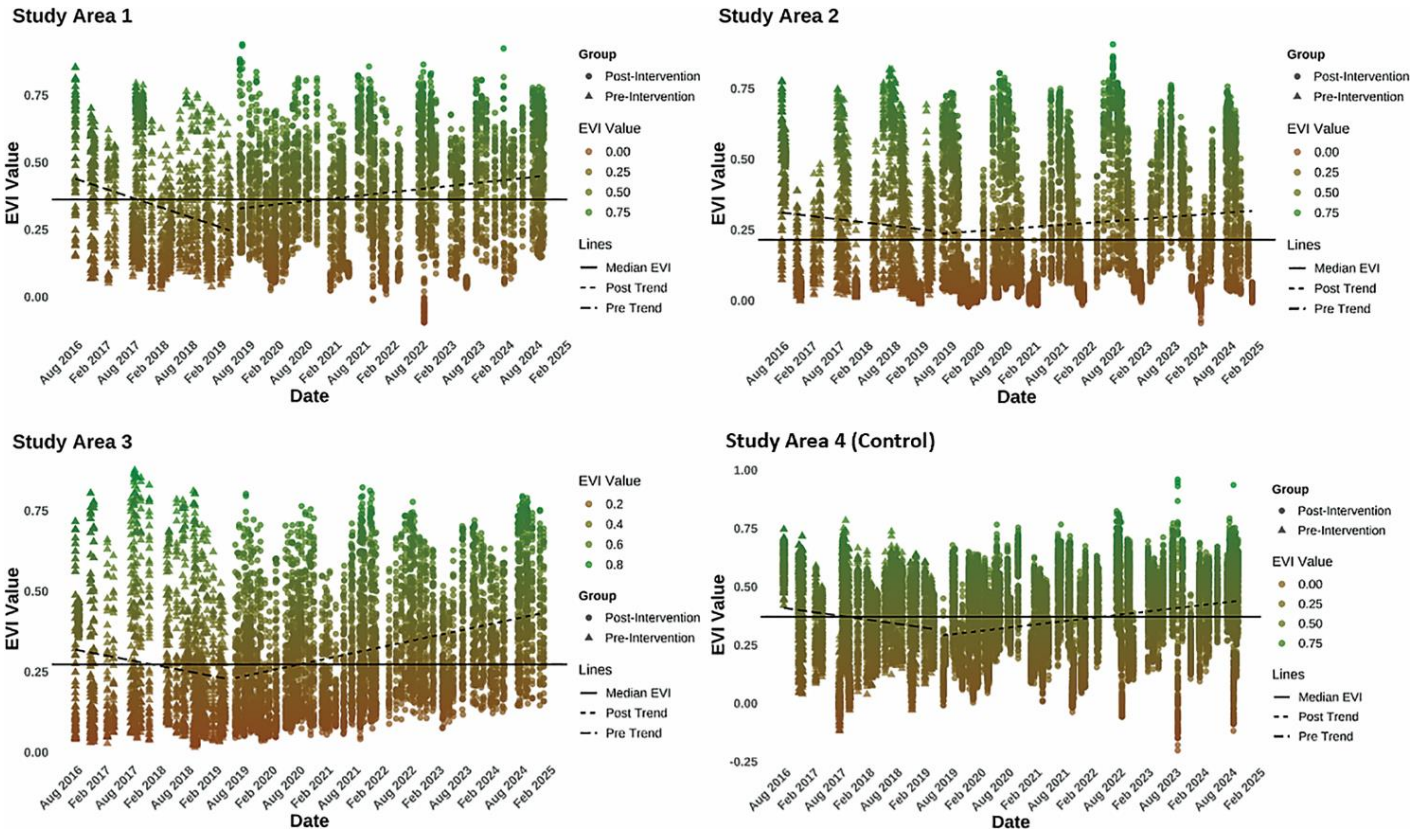

Figure 6 • Scatter plots displaying the temporal trends of the Enhanced Vegetation Index (EVI) for Study Areas 1–3 and the Control Area from August 2016 to December 2024. Each point represents an individual EVI observation, with color coding from brown (low vegetation) to green (high vegetation) to indicate vegetation health over time. To evaluate vegetation changes in response to the intervention, separate linear trend lines were fitted for the pre-intervention (2017–2019) and post-intervention (August 2019–2024) periods. Additionally, a median line was fitted for each period to establish a baseline for trend comparisons over time. In Study Area 1, a gradual upward trend in post-intervention EVI values is observed, with a noticeable shift in the post-intervention median EVI compared to the pre-intervention median. Study Area 2 exhibits a similar pattern, though the increase in EVI is more variable. Study Area 3 exhibits a clear upward trend in post-intervention EVI values, with a significant rise in the median EVI compared to the pre-intervention period. This suggests a steady and consistent recovery, indicating a positive vegetation response to the intervention. The Control Area provides a baseline comparison, where the trend line remains relatively flat, and the post-intervention median EVI shows little to no change compared to the pre-intervention median. Overall, these results indicate that vegetation recovery is more evident in the treated study areas, with varying degrees of effectiveness, whereas the control site remains stable.

Lastly, in the Control Area, as shown in Figure 5, the pre-treatment period is characterized by relatively stable but lower EVI values, with a slight downward trend, indicating minimal vegetation growth over time. Throughout this period, a significant proportion of EVI values remains below the median reference line, suggesting that vegetation cover was sparse and exhibited limited natural regeneration. Unlike the intervention sites, this area did not receive any active revegetation efforts, serving as a baseline for assessing natural vegetation trends. Over time, there is no substantial shift in EVI distribution, and while the post-period trend line exhibits a slight positive trajectory, the magnitude of change is minimal. Some green-colored points emerge in later years, indicating localized improvements in vegetation health, but overall, EVI values continue to fluctuate without a clear upward shift. The persistence of these fluctuations suggests that natural regrowth was inconsistent, with some areas experiencing minor improvements while others remained unchanged or continued to degrade.

4. Discussion

Our findings indicate that drone-facilitated vegetation interventions can effectively enhance post-landslide recovery, as demonstrated in Study Areas 1 and 3, where EVI values improved markedly following the intervention. This conclusion is supported by both the long-term Landsat NDVI analysis—capturing nearly two decades of data—and the more granular Sentinel-2 EVI assessments. Notably, Study Area 1 showed particularly pronounced gains in its central regions, whereas Study Area 3 exhibited localized improvements around the periphery. These observations were further reinforced by the outcomes of the K-S test, ECDF, and PDF analyses, which consistently indicated a significant post-intervention rise in vegetation health.

Moreover, the success of these interventions aligns with previous work in Taiwan, which found that vegetation recovery after landslides depends on multiple environmental factors. Soil moisture, for instance, is integral for plant establishment, aiding both growth and slope stabilization [27, 28]. Precipitation levels can facilitate plant development while also triggering further landslides, creating a dual effect that is especially evident in the first few years after a landslide [29, 30]. Topographic features, such as elevation and slope inclination, also play a notable role: recovery tends to be weaker at very low (<1,300 m) and high elevations (>3,300 m) and on gentler slopes (<35°) compared to steeper slopes (>35°) [30, 31, 32]. Additionally, native pioneer

species like *Arundo formosana* and *Pinus taiwanensis* can expedite successional processes and are particularly valuable in steep or exposed locations [31, 33].

By contrast, Study Area 2 did not experience a similar level of improvement. Its 14-year gap between the major landslide and the drone-based seeding suggests that substantial natural recovery had already taken place, potentially minimizing any observable benefits of the drone intervention. Sentinel-2 data from this site revealed a negative EVI trend prior to the drone initiative, followed by a relatively flat trend afterward, indicating limited improvement attributable to the intervention. The ECDF and PDF analyses support this, showing a discernible shift toward lower EVI values post-intervention. These findings highlight the importance of both timing and environmental conditions; when drone seeding efforts are introduced after a lengthy period of natural regeneration, the intervention may be neither necessary nor impactful.

Meanwhile, the Control Area, which did not receive any drone-facilitated intervention, exhibited minimal natural recovery in EVI compared to the improvements observed in Study Areas 1 and 3. Although a degree of successional regrowth did occur, it was modest, reinforcing the potential limitations of relying on passive restoration in remote or highly disturbed environments. The relatively small distributional shift in EVI at the control site further contrasts with the larger, more statistically significant gains seen in areas where drone seeding was applied, underscoring the advantages of active intervention.

5. Conclusions

In conclusion, when viewed in the broader context of the research question "Does drone-facilitated revegetation work?", our results suggest that UAV-based aerial seeding can indeed be an effective method, provided that seed design and environmental parameters are carefully aligned. Additionally, monitoring vegetation health by analyzing Enhanced Vegetation Index (EVI) and Normalized Difference Vegetation Index (NDVI) can provide valuable insights for such UAV-based methods. Although Study Area 2 exhibited suboptimal outcomes, the approach's relative advantages in cost, safety, and coverage across rugged terrain underscore its value for ecosystem restoration. Future studies could refine drone seeding strategies by incorporating site-specific ecological conditions, such as seed mix selection, timing, and environmental constraints like slope or soil type. Continued monitoring over extended periods is crucial for evaluating the stability of revegetated areas and for comparing drone seeding to other restoration techniques, including manual planting or helicopter seeding. Ultimately, the ability to balance revegetation efficacy, cost-effectiveness, and logistical feasibility presents a compelling case for drone-based restoration efforts in landslide-prone regions.

Funding

The authors declare no financial support for the research, authorship, or publication of this article.

Author contributions

Conceptualization, S.F. and M.L.; methodology, M.G.S. and M.L.; formal analysis, M.G.S.; writing—original draft preparation, S.F. and M.L.; writing—review and editing, S.F. and M.G.S.; visualization, M.G.S.; supervision, S.F. and M.G.S.; project administration, S.F. All authors have read and agreed to the published version of the manuscript.

Conflict of interest

The authors declare no conflict of interest.

Data availability statement

Data supporting these findings are available within the article, at https://doi.org/10.20935/AcadEnvSci7624, or upon request.

Institutional review board statement

Not applicable.

Informed consent statement

Not applicable.

Additional information

Received: 2024-07-23

Accepted: 2025-03-17

Published: 2025-04-07

Academia Environmental Sciences and Sustainability papers should be cited as *Academia Environmental Sciences and Sustainability 2025*, ISSN 2997-6006, https://doi.org/10.20935/AcadEnvSci7624. The journal's official abbreviation is *Acad. Env. Sci. Sust.*

Publisher's note

Copyright

References

1. Van Andel J, Aronson J, editors. Restoration ecology: the new frontier. Oxford: John Wiley & Sons; 2012.
2. Atyeo C, Thackway R. Mapping and monitoring revegetation activities in Australia–towards national core attributes. Australas J Environ Manag. 2009;16(3):140–8. doi: 10.1080/14486563.2009.9725230

3. Laarman J. Seeding from aircraft: an appropriate technology for reforestation?. Int Tree Crops J. 1984;3(1):63–73. doi: 10.1080/01435698.1984.9752774

4. Sivakumar V, Anandalakshmi R, Warrier RR, Singh BG, Subramanian K. Seed pelleting and aerial seeding. In: Vanangamudi K, Kalaivani S, Vanangamudi M, Sastry G, Selvakumari A, Srimathi P, editors. Seed quality enhancement: principles and practices. Jodhpur: Scientific Publishers; 2010. p. 207.

5. Robinson JM, Harrison PA, Mavoa S, Breed MF. Existing and emerging uses of drones in restoration ecology. Methods Ecol Evol. 2022;13:1899–911. doi: 10.1111/2041-210X.13912

6. Mohan M, Richardson G, Gopan G, Aghai MM, Bajaj S, Galgamuwa GP, et al. UAV-supported forest regeneration: current trends, challenges and implications. Remote Sens. 2021;13(13):2596. doi: 10.3390/rs13132596

7. Castro J, Morales-Rueda F, Alcaraz-Segura D, Tabik S. Forest restoration is more than firing seeds from a drone. Restor Ecol. 2023;31(1):e13736. doi: 10.1111/rec.13736

8. Lohit GVS. Reforestation using drones and deep learning techniques. In 2021 7th International Conference on Advanced Computing and Communication Systems (ICACCS); 2021 Mar 19–20; Coimbatore, India. Vol. 1. IEEE; 2021. p. 847–52.

9. Hsu K-C, Song G-ZM, Lin S-H, Shiau H-M. Operation methods and applications for revegetating landslides with UAVs. J Chin Soil Water Conserv. 2021;52:16–26. doi: 10.29417/JCSWC.202103_52(1).0002

10. Forestry Bureau Council of Agriculture. Feasibility evaluation for UAV seeding vegetation pellets on the landslide of national forest. Achievements Report; 2019 [cited 2025 Jan 19]. Available from: https://yilan.forest.gov.tw/research/0003887

11. Zong-Ren H, Kun-Sheng Y. Discussion on the Development of UAV Technology and Its Application in Forestry. [cited 2025 Jan 19]. [In Chinese]. Available from: https://kmweb.moa.gov.tw/knowledgebase.php?id=389676

12. Hsu K-C, Song G-ZM, Lin S-H, Chang C-H. Feasibility evaluation for unmanned-aerial-vehicle seeding on post landslide sites in Taiwan. In: Chia C, editor. Scour and erosion IX. London: Taylor & Francis Group; 2018. p. 583–90.

13. Liao G. Taiwan revegetates landslide areas by using drones to drop seeds. Taiwan News; 2019 [cited 2022 Dec 1]. Available from: https://www.taiwannews.com.tw/news/3711829

14. Liao J. Afforestation in the collapsed water catchment area relies on the new technology of drones, but the airdrop of foreign grass seeds is controversial. Environmental Information Center; 2019 cited 2022 Dec 1]. Available from: https://e-info.org.tw/node/218235

15. Datong Township Government. Yilan County Regional disaster prevention and relief plan. Central Disaster Prevention and Relief Council; 2018 [cited 2025 Jan 19]. Available from: https://cdprc.ey.gov.tw/Page/C10B9C4A41D6D55F/eae12a31-2c1f-4283-b947-66c58b28cbe9

16. Juang CS, Stanley TA, Kirschbaum DB. Using citizen science to expand the global map of landslides: introducing the Cooperative Open Online Landslide Repository (COOLR). PLoS One. 2019;14(7):e0218657. doi: 10.1371/journal.pone.0218657

17. Mutanga O, Kumar L. Google earth engine applications. Remote Sens. 2019;11:591. doi: 10.3390/rs11050591

18. Leidman SZ, Rennermalm ÅK, Lathrop RG, Cooper MG. Terrain-based shadow correction method for assessing supraglacial features on the Greenland ice sheet. Front Remote Sens. 2021;2:20. doi: 10.3389/frsen.2021.690474

19. Streutker DR, Glenn NF, Shrestha R. A slope-based method for matching elevation surfaces. Photogramm Eng Remote Sens. 2011;77:743–50. doi: 10.14358/PERS.77.7.743

20. Teillet PM, Guindon B, Goodenough DG. On the slope-aspect correction of multispectral scanner data. Can J Remote Sens. 1982;8:84–106. doi: 10.1080/07038992.1982.10855028

21. Gurung RB, Breidt FJ, Dutin A, Ogle SM. Predicting Enhanced Vegetation Index (EVI) curves for ecosystem modeling applications. Remote Sens Environ. 2009;113:2186–93. doi: 10.1016/j.rse.2009.05.015

22. Huete A, Didan K, Miura T, Rodriguez EP, Gao X, Ferreira LG. Overview of the radiometric and biophysical performance of the MODIS vegetation indices. Remote Sens Environ. 2002;83:195–213. doi: 10.1016/S0034-4257(02)00096-2

23. Landsat Missions. Landsat enhanced vegetation index. USGS; 2023 [cited 2024 Apr 2]. Available from: https://www.usgs.gov/landsat-missions/landsat-enhanced-vegetation-index

24. Pettorelli N, Vik JO, Mysterud A, Gaillard JM, Tucker CJ, Stenseth NC. Using the satellite-derived NDVI to assess ecological responses to environmental change. Trends Ecol Evol. 2005;20(9):503–10. doi: 10.1016/j.tree.2005.05.011

25. Zeng Q, Lu X, Chen S, Cui X, Zhang H, Zhang Q. Comparing the performance of vegetation indices for improving urban vegetation GPP estimation via eddy covariance flux data and Landsat 5/7 data. Ecol Inform. 2025;86:103023. doi: 10.1016/j.ecoinf.2025.103023

26. Massey Jr FJ. The Kolmogorov-Smirnov test for goodness of fit. J Am Stat Assoc. 1951;46:68–78. doi: 10.1080/01621459.1951.10500769

27. Lin C, Lo H, Chou W, Lin W. Vegetation recovery assessment at the Jou-Jou Mountain landslide area caused by the 921 Earthquake in Central Taiwan. Ecol Model. 2004;176:75–81. doi: 10.1016/J.ECOLMODEL.2003.12.037

28. Lin W, Chou W, Lin C, Huang P, Tsai J. Vegetation recovery monitoring and assessment at landslides caused by earthquake in Central Taiwan. Forest Ecol Manag. 2005;210:55–66. doi: 10.1016/J.FORECO.2005.02.026

29. Yang M, Chen S, Tsai H. A long-term vegetation recovery estimation for Mt. Jou-Jou using multi-date SPOT 1, 2, and 4 images. Remote Sens. 2017;9:893. doi: 10.3390/rs9090893

30. Yang W, Qi W, Zhou J. Effects of precipitation and topography on vegetation recovery at landslide sites after the 2008 Wenchuan earthquake. Land Degrad Dev. 2018;29:3355–65. doi: 10.1002/ldr.3098

31. Lin W, Chou W, Lin C. Earthquake-induced landslide hazard and vegetation recovery assessment using remotely sensed data and a neural network-based classifier: a case study in central Taiwan. Nat Hazards. 2008;47:331–47. doi: 10.1007/S11069-008-9222-X

32. Zhong C, Li C, Gao P, Li H. Discovering vegetation recovery and landslide activities in the Wenchuan earthquake area with Landsat imagery. Sensors. 2021;21:5243. doi: 10.3390/s21155243

33. Chou W, Lin W, Lin C. Vegetation recovery patterns assessment at landslides caused by catastrophic earthquake: a case study in central Taiwan. Environ Monit Assess. 2009;152:245–57. doi: 10.1007/s10661-008-0312-8